




## Constructing inverse scattering potentials for charged particles using a reference potential approach

O. S. K. S. Sastri <sup>\*</sup>, Arushi Sharma <sup>†</sup> and Ayushi Awasthi <sup>†</sup>

*Department of Physics and Astronomical Sciences, Central University of Himachal Pradesh, Dharamsala, Bharat (India) 176215, India*



(Received 17 November 2023; revised 27 March 2024; accepted 28 May 2024; published 18 June 2024)

An accurate way to incorporate long-range Coulomb interaction alongside short-range nuclear interaction has been a challenge for theoretical physicists. In this paper, we propose a methodology based on the reference potential approach for constructing inverse potentials for charged particle scattering. The central idea is to obtain the inverse potential directly from the expected scattering phase shifts by comparing them with those obtained by solving the phase equation for a chosen reference potential. The design of the reference potential is key to incorporating the Coulomb interaction successfully. Here, a combination of two smoothly joined Morse functions, one regular followed by an inverted one, is considered. While the former takes care of short-range nuclear and Coulomb interactions, the latter accounts for expected barrier height due to the long-range Coulomb part that dominates once nuclear interaction subsides. The final step is to incorporate the phase equation within an iterative loop of an optimization algorithm to obtain the model parameters for the reference potential by minimizing the mean absolute percentage error between the obtained and expected scattering phase shifts. We have applied the methodology to the  $\alpha - \alpha$  system and constructed the inverse potentials for its  $S$ ,  $D$ , and  $G$  states with mean absolute percentage errors of 0.9, 0.5, and 0.4 respectively. Their respective resonances (experimental), in MeV, are found to be at 0.1240 (0.0918), 2.95 (3.03), and 11.89 (11.35). One can conclude that the reference potential approach using a combination of smoothly joined Morse functions is successful in accurately accounting simultaneously for the short-range nuclear and the long-range Coulomb interactions between charged particles in nuclear scattering studies.

DOI: [10.1103/PhysRevC.109.064004](https://doi.org/10.1103/PhysRevC.109.064004)

### I. INTRODUCTION

The key to scattering phenomena is to model the underlying interaction potential that gives rise to the scattering phase shifts (SPS) that are responsible for the observed experimental scattering cross sections. The theoretical approaches [1–3] most often utilized rely upon determination of the scattering phase shift from the wave function that is obtained by solving the time independent Schrödinger equation (TISE). The potential is chosen by modeling the interactions primarily due to nuclear and Coulomb forces and, in some cases, by adding perturbation terms due to the interplay of spin, isospin, and orbital angular momentum. These potentials are typically represented by various mathematical functions that best represent the nature of the interaction as can be elicited from the phase shift values and the trends they follow at different laboratory energies [4]. An alternative approach is to rephrase the second order TISE as a first order nonlinear Riccati equation for different  $\ell$  channels as in the phase function method [5,6]. One advantage of this latter method is that it deals with the interaction potential directly, eliminating the requirement for a wave function. This enables the construction of inverse

potentials directly from the available experimental data, as in inverse scattering theory [7].

Theoretically, constructing inverse potentials [8] requires not only information regarding all the bound state energies  $E_n$  ( $n = 0, 1, \dots, N$ ) along with their related normalization constants  $C_n$  but also the phase shifts for all scattering energies  $E > 0$  ranging to infinity. Most often, phase shift data are available for only certain energies within a limited range and hence a rigorous solution of the quantum mechanical inverse problem is extremely difficult to compute. The inverse problem is akin to the machine learning (ML) paradigm wherein one obtains the model of interaction from large amounts of available data. Typically, one prefers neural-network-based models [9], when the number of available experimental data is very large, say  $\geq 1000$ . Otherwise, it is more appropriate to use metaheuristic algorithms [10–12] as part of these ML models and enhance their performance by incorporating the knowledge of the problem from the physics that underlies the phenomenon.

Selg [13] proposed using Morse functions as the zeroth reference to obtain the scattering phase shift, and went on to solve the Marchenko integral equation that gives rise to the inverse potential. We proposed a computational approach to construct inverse potentials [4,7] for nucleon-nucleon by utilizing a single Morse function as a reference. Although this method is effective in calculating the inverse potentials for scattering in scenarios where the projectile or target particles

<sup>\*</sup> Also at IUAC, New Delhi; Contact author: [sastri.osks@hpcu.ac.in](mailto:sastri.osks@hpcu.ac.in)

<sup>†</sup> These authors contributed equally to this work.

are both neutral, charged systems necessitate the addition of a Coulomb potential. Incorporating the long-range Coulomb interactions remains a challenge to theoretical physicists even today. Most often, screened Coulomb potentials are utilized, since in experiments an isolated charge is generally surrounded by residual particles due to polarization.

Taylor [14] presented a comprehensive method of incorporating Coulomb scattering by considering

$$V_c^\rho(r) = \frac{\gamma}{r} \alpha^\rho(r),$$

where the screening function  $\alpha^\rho$  for a given  $\rho$  must go to zero as  $r$  tends to  $\infty$  and must approach 1 as  $\rho$  tends to  $\infty$  with  $r$  fixed. As long as  $\rho$  is very large, such a potential meets the conditions of scattering theory and produces findings that are independent of both properties of screened potentials: their nature/shape and screening radius. Ali-Bodmer [15], Buck [16] and Odsuren [17] utilize an erf() function to model the Coulomb interaction [18]. Laha *et al.* utilize screened Coulomb interaction based on the atomic Hulthen [19] potential. Previously, while studying  $p$ - $p$  [20],  $p$ - $d$  [21],  $p$ - $\alpha$  [22], and  $\alpha$ - $\alpha$  [18,23] systems, we also chose to incorporate the erf() based Coulomb potential. To get accurate scattering phase shifts, we cut off the erf() at a certain distance  $r_f$  abruptly, which is a major limitation of this approach. Recently, we undertook a study of  $\alpha$ - $\alpha$  scattering using various phenomenological potentials by utilizing the atomic Hulthen potential as the screened Coulomb potential [24]. It was observed that the screening radius had to be varied for different  $\ell$  channels to obtain a good match with experimental data. Hence, there is a need for an *Ansatz* that can effectively incorporate the long-range Coulomb potential in charged particle scattering.

To solve this crucial issue we focused on the  $\alpha$ - $\alpha$  scattering reaction, which has great importance in stellar astrophysics [25] and also in understanding the Hoyle state in  $^{12}\text{C}$  [26]. Current research on  $\alpha$ - $\alpha$  scattering involves nuclear lattice effective field theory (NLEFT) alongside lattice QCD calculations [26,27]. To account for long-range Coulomb interaction in  $\alpha$ - $\alpha$  scattering [25], a Coulomb-modified effective range expansion from next-to-leading order (NLO) onwards is utilized and lattice calculations are performed in a box of 100–120 fm<sup>3</sup> [25,26] using the adiabatic projection method, by assuming that it is far beyond the strong interaction range. Even these *ab initio* calculations are still having difficulties dealing with long-range Coulomb interaction, which tends to tremendously increase the computational time due to large box sizes [28].

A further review of the literature revealed an interesting approach suggested by Selg [29,30], where the molecular interaction potentials were obtained by considering a combination of two or three Morse functions. The key advantage of this approach is the low number of analytically distinct components required to provide a decent match with the original potential across a broad distance range. In this paper, our goal is to obtain the inverse potential without taking recourse to Coulomb interaction.

The specific objective of this study is to develop inverse potentials by examining elastic scattering of charged  $\alpha$

particles with  $^4\text{He}$  having orbital angular momentum  $l = 0, 2, 4$  at energies up to 28.5 MeV, utilizing a combination of two Morse potentials across two distinct regions.

## II. REFERENCE POTENTIAL APPROACH

Selg [13,31] suggested a combination of smoothly joined Morse potentials as a starting point to solve the time-independent Schrödinger equation for its energy eigenvalues, scattering phase shifts, and also Jost function, from which one can obtain the inverse potential [30].

In this paper, we utilize only two Morse components to prepare the reference potential.

$$V_{\text{RPA}}(r) = \begin{cases} V_{\text{NC}} & \text{if } r \leq X, \\ V_{\text{CL}} & \text{if } r \geq X, \end{cases} \quad (1)$$

where

$$V_{\text{NC}} = V_1 + D_1[e^{-2\alpha_1(r-r_1)} - 2e^{-\alpha_1(r-r_1)}]. \quad (2)$$

$V_{\text{NC}}$  is a regular Morse component, which accounts for short-range nuclear and Coulomb interactions, and

$$V_{\text{CL}} = V_2 - D_2[e^{-2\alpha_2(r-r_2)} - 2e^{-\alpha_2(r-r_2)}]. \quad (3)$$

$V_{\text{CL}}$  is a reversed Morse component for incorporating long-range Coulomb interaction.

Here  $D_k$  are potential depths at equilibrium distances  $r_k$ , and  $\alpha_k$  reflect shape parameters of Morse functions respectively.  $V_k$  are constants added to the total potential. These functions are smoothly joined at boundary points  $X$ . The number of distinct Morse-type components that may be added is almost unlimited. Naturally, the more components one includes, the better the match with the experimental data, but also the more challenging the analytical solution to the problem gets. Note that as  $r_2$  tends to infinity the Coulomb barrier height approaches zero.

To ensure smoothness of potential at the boundary point  $X$ , in between the two functions, the functions and their derivatives must be continuous at  $X$ . That is

$$\begin{aligned} V_{\text{NC}}(r)|_X &= V_{\text{LC}}(r)|_X, \\ \frac{dV_{\text{NC}}(r)}{dr}|_X &= \frac{dV_{\text{LC}}(r)}{dr}|_X. \end{aligned} \quad (4)$$

Using these equations, two of the eight parameters were determined as

$$D_1 = \frac{(V_2 - V_1)\alpha_2 f_2}{\alpha_2 f_3 f_2 - \alpha_1 f_4 f_1}, \quad (5)$$

$$D_2 = \frac{(V_1 - V_2)\alpha_1 f_1}{\alpha_2 f_3 f_2 - \alpha_1 f_4 f_1}, \quad (6)$$

where

$$\begin{aligned} f_1 &= e^{-2\alpha_1(r-r_1)} - e^{-\alpha_1(r-r_1)}, \\ f_2 &= e^{-2\alpha_2(r-r_2)} - e^{-\alpha_2(r-r_2)}, \\ f_3 &= e^{-2\alpha_1(r-r_1)} - 2e^{-\alpha_1(r-r_1)}, \\ f_4 &= e^{-2\alpha_2(r-r_2)} - 2e^{-\alpha_2(r-r_2)}. \end{aligned}$$

Now, observing Eqs. (5) and (6), one can see that not choosing  $V_1$  and  $V_2$  would have led to two homogeneous equations and

determination of  $D_1$  and  $D_2$  would not have been feasible. The reference potential is a family of curves with a total of seven parameters, including boundary point  $X$ . While Selg [32] obtains analytical expressions for energies and phase shifts by solving radial Schrödinger equation for molecular potentials, we take an alternative computational approach by employing the phase function method.

### III. PHASE FUNCTION METHOD

The phase function method is one of the important tools in scattering studies for both local [5] and nonlocal interactions [33,34]. The second-order time-independent Schrödinger equation for a potential  $U(r)$ ,

$$\frac{\partial^2 \psi(r)}{\partial r^2} + \frac{2m}{\hbar^2} [E - U(r)] \psi(r) = 0, \quad (7)$$

is recast into a first-order nonlinear differential equation of Riccati type,

$$\frac{d\delta_l(k, r)}{dr} = -\frac{U(r)}{k} \{ \hat{j}_l(kr) \cos[\delta_l(k, r)] - \hat{\eta}_l(kr) \sin[\delta_l(k, r)] \}^2, \quad (8)$$

where  $k_{c,m} = \sqrt{2\mu E_{c,m}/\hbar^2}$ ,  $U(r) = 2\mu V(r)/\hbar^2$ , and  $\hat{j}_l(kr)$  and  $\hat{\eta}_l(kr)$  are the Riccati-Bessel and Riccati-Neumann functions, respectively. For the  $\alpha - \alpha$  system,  $\hbar^2/2\mu = 10.44217$  MeV fm<sup>2</sup>.

This gives phase shift information at various energies by directly taking the potential as input. For  $\ell = 0, 2, 4$  states, the corresponding phase equations [18] can be obtained by substituting the appropriate  $\ell$ th-order Riccati-Bessel and Riccati-Neumann functions as

(1)  $\ell = 0$ :

$$\delta'_0(k, r) = -\frac{U(r)}{k} \sin^2[\delta_0 + kr]; \quad (9)$$

(2)  $\ell = 2$ :

$$\delta'_2(k, r) = -\frac{U(r)}{k} \left[ -\sin(\delta_2 + kr) - \frac{3 \cos(\delta_2 + kr)}{kr} + \frac{3 \sin(\delta_2 + kr)}{kr^2} \right]^2; \quad (10)$$

(3)  $\ell = 4$ :

$$\delta'_4(k, r) = -\frac{U(r)}{k} \left[ \sin(\delta_4 + kr) + \frac{10 \cos(\delta_4 + kr)}{kr} - \frac{45 \sin(\delta_4 + kr)}{kr^2} - \frac{105 \cos(\delta_4 + kr)}{kr^3} + \frac{105 \sin(\delta_4 + kr)}{kr^4} \right]^2. \quad (11)$$

These equations are solved using the fifth-order Runge-Kutta (RK-5) method by choosing the initial condition as  $\delta_\ell(0, k) = 0$ . The final integration point is chosen in such a way that total potential becomes negligible at large distances. The model parameters of the chosen potential are optimized by iteratively solving the phase equations for various energies

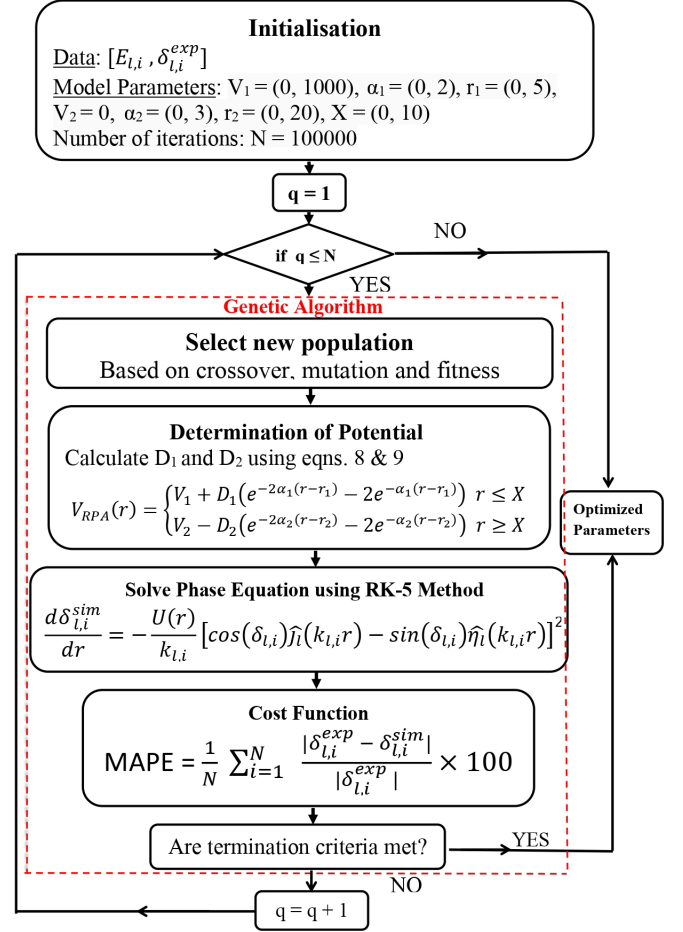


FIG. 1. Flowchart of the optimization procedure.

and minimizing mean absolute percentage error (MAPE), between computed and experimental scattering phase shifts. In our work, we have utilized a genetic algorithm to converge to the best solutions.

### IV. OPTIMIZATION PROCEDURE

One can optimize the model parameters of the chosen potential by iteratively solving the phase equations for various energies and minimizing a cost function. Typically, one can employ mean squared error, mean absolute percentage error (MAPE),  $\chi^2$  error, etc., between computed and experimental scattering phase shifts, as cost functions. In our work, we have utilized a genetic algorithm, as it can converge to a global minimum and not get stuck in local minima regions [11,35]. The flowchart for the optimization procedure followed by us is shown in Fig. 1.

- (1) *Initialization Step*: First arrays for the energies and corresponding scattering phase shifts are created. Then, the bounds for various model parameters that need to be optimized are chosen. One can also simultaneously give as input one of the previously obtained parameter sets to be included in the population.

- (2) *Genetic algorithms* [36]: These typically create random populations [11,37], which represent possible candidate solutions called parents, from the sample space specified by the chosen bounds for various model parameters.
- (3) *Determination of potential*: The reference potentials corresponding to each of the parameters generated as parent class are determined.
- (4) *Solving phase equation for various energies*: For each of the input potentials the phase equation, corresponding to a particular orbital angular momentum  $\ell$ , is solved using the the fifth-order Runge-Kutta method for different energies. The obtained scattering phase shifts are utilized to determine the cost function, which is compared with expected phase shifts from experiments.
- (5) *Termination criteria*: If after many iterations, there is no further improvement in the minimization of cost function due to all considered candidate solutions, the genetic algorithm exits and provides the best possible solution. Otherwise, it creates new candidate solutions by adding a mutation and crossover based on fitness assignment and the iterations continue till the end [37].

This type of optimization procedure is typically referred to as a metaheuristic algorithm and is often used in machine learning paradigms where one obtains the model from the available data. These genetic algorithms have the best parallel capabilities and provide a solution for a problem that improves over time. It helps in optimizing various problems such as discrete functions, multi-objective problems, and continuous functions. This is the motivation for choosing genetic algorithms over traditional algorithms.

Since the optimization procedure involves the generation of random populations, the runs might lead to slightly different model parameters on convergence to a similar MAPE value. Hence, it is necessary to run the code with the same initial bounds for various model parameters multiple times, and their average values and respective uncertainties are computed [36].

## V. RESULTS

### A. Experimental data

The updated database for  $\alpha - \alpha$  scattering by Anil *et al.*, [18] had included the Chein and Brown data [38] for energies up to 25.5 MeV only, wherein  $\ell = 4$  has only four data points. Since there are seven model parameters, we have selected experimental data points, for all the  $\ell$  channels, up to 28.5 MeV, which is just about the threshold binding energy of  $\alpha$  particles.

### B. Physical considerations

While constructing inverse potentials for  $\alpha - \alpha$  system, the following physical considerations play an important role:

- (1) The Coulomb barrier  $V_{CB}$  for the  $\ell = 0$  potential needs to be close to 0.0918 MeV, the resonant scattering due to the pseudobound state.

- (2) After accounting for centrifugal potential, the depth of the  $\ell = 2$  potential must be lower than that of the  $\ell = 0$  potential, and the Coulomb barrier height  $V_{CB}$  must be on the order of resonance energy, which has been measured to be  $\approx 3$  MeV.
- (3) Similarly, the depth of the  $\ell = 4$  potential must be less than that of  $\ell = 2$  and  $V_{CB}$  of  $\approx 12$  MeV.

### C. Optimization of model parameters

- (1) In our current analysis, we have opted to use a combination of two Morse potentials over the entire region of interest. For the first part of the region,  $0 \leq r \leq X$ , it is a regular Morse with four parameters, and the second part for larger distances,  $X \leq r \leq r_f$ , has an inverse Morse function with another four parameters. These two together have to produce a smooth-shaped potential that accounts for the observed scattering phase shifts. So, employing continuity conditions as given in Eqs. (4), one obtains the two parameters  $D_1$  and  $D_2$  in terms of the rest of the parameters as given by Eqs. (5) and (6). This reduces the number of parameters required to 6 but one needs to fix the point  $X$  as well. So, observing that the relative difference  $V_1 - V_2$  appears in both Eqs. (5) and (6), we chose to set  $V_2 = 0$ . In fact, we initially ran the optimization routine by fixing different values of  $X$  and observed that  $V_2$  always came out to be of the order of  $10^{-8}$ . So, in this way, we came to the conclusion that only six parameters need to be determined.
- (2) Initially, the bounds on each of the six parameters are chosen to cover a wide range, and the final integration distance  $r_f$  is set to 80 fm. Then, we execute the optimization code, which iteratively calls the RK-5 routine for determining SPS, till the mean absolute percentage error converges to a minimum value. It was observed that the potentials die down to zero within 40 fm. Hence, we set  $r_f = 40$  fm for the rest of the runs.
- (3) Then, the bounds are adjusted to ensure that the resultant inverse potential is physically relevant satisfying the conditions, as stated above. In this sense, our machine-learning-based heuristic algorithm not only utilizes the phase equation that governs the scattering phenomenon but also takes input on the bounds that need to be set for the model parameters to result in a physically acceptable interaction potential.
- (4) By fixing these bounds, the optimization code was run for various initial seeds. The convergence achieved in these runs resulted in interaction potentials that are very close to each other. The mean absolute percentage error values obtained at convergence differ only at the third decimal place. Thus, the stability and reliability of the code is established.
- (5) The final optimized parameters with average values along with uncertainties for various  $\ell$  channels are given in Table I. The MAPE values shown are only to the first decimal place.



TABLE I. Optimized model parameters for  $\alpha - \alpha$  scattering. The  $\pm$  values given are obtained by multiple runs of the code.

Model Parameters	$\ell = 0$	$\ell = 2$	$\ell = 4$
$\alpha_1$	$0.1289 \pm 0.0291$	$0.7693 \pm 0.0812$	$0.2968 \pm 0.0867$
$r_1$	$4.5649 \pm 0.0500$	$1.4975 \pm 0.1028$	$0.4562 \pm 0.2652$
$\alpha_2$	$0.3884 \pm 0.0077$	$2.5310 \pm 0.1338$	$0.8197 \pm 0.0031$
$r_2$	$11.9329 \pm 0.0187$	$4.6301 \pm 0.0419$	$7.7862 \pm 0.0318$
X	$6.0825 \pm 0.0501$	$4.5239 \pm 0.0580$	$2.6297 \pm 0.0250$
MAPE	0.9	0.5	0.4

#### D. Scattering phase shifts and inverse potentials

The obtained SPS using the model parameters in Table I, along with the expected SPS from [18,38], have been plotted in Fig 2. One can observe that all the obtained SPS are well within the error bars of the expected ones. The MAPE values for SPS of  $\ell = 0, 2, 4$  channels are found to be 0.9, 0.5, and 0.4 respectively, and are currently the best fits to the expected data.

The constructed inverse potentials for  $\ell = 0, 2, 4$  channels are plotted without and with centrifugal potential in Figs. 3(a) and 3(b) respectively. The important features of these potentials are their depth  $V_d$  at  $r_1$  which specifies maximum attraction and Coulomb barrier height  $V_{CB}$  at  $r_2$ . These are referred to as interaction parameters. It is to be noted that the optimized model parameters do not directly reflect the nature of the interaction. The values of interaction parameters  $V_d$  and  $V_{CB}$  are obtained from the potential that includes the centrifugal term at distances  $r_1$  and  $r_2$  respectively. The determined  $V_d$

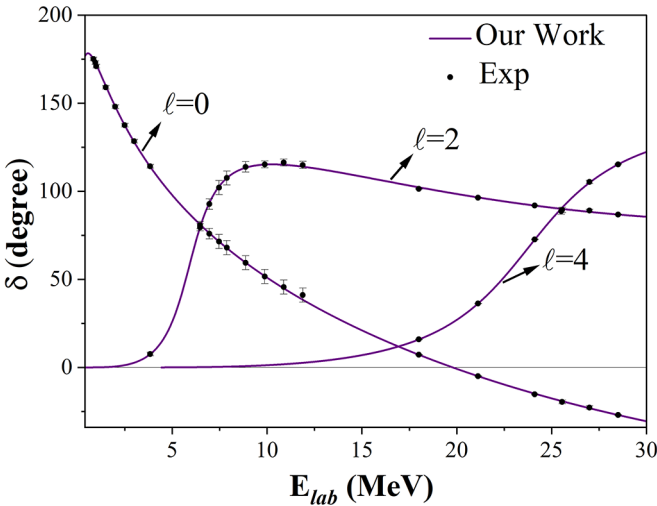


FIG. 2.  $\alpha - \alpha$  scattering phase shifts for  $\ell = 0, 2$ , and  $4$  channels obtained using the Reference Potential Approach (RPA) along with expected data [18,38].

TABLE II. Interaction parameters for  $\alpha - \alpha$  scattering obtained from inverse potentials after adding the centrifugal term.

Model Parameters	$\ell = 0$	$\ell = 2$	$\ell = 4$
$V_d$	$-10.8604 \pm 0.2581$	$-4.3951 \pm 0.2785$	$-0.0127 \pm 0.2149$
$V_{CB}$	$0.0839 \pm 0.0059$	$4.9653 \pm 0.1103$	$11.1652 \pm 0.0057$

and  $V_{CB}$  for  $\ell = 0, 2, 4$  channels are presented in Table II. The scattering phase shift for  $\ell = 0$  becomes negative beyond 20 MeV. This is reflected in the value of the repulsive core with  $V_r = 85-95$  MeV. This value obtained by other *Ansätze* for the screened Coulomb potential based on erf() [18] and atomic Hulthen potential [24] was found to be 406 and 619 MeV respectively, which are very large. The Coulomb repulsion giving rise to barrier height for  $\ell = 0$  is shown as an inset in Fig. 3(a). One can also observe that the experimentally observed resonance at 0.0918 MeV falls within the range of  $V_{CB}$  values obtained by the reference potential approach. This clearly brings out the pseudobound state structure of  $^8\text{Be}$ . The potential goes close to zero, to an order of  $10^{-4}$  MeV, at a distance  $r_c$ , called a cutoff, and is found to be 33.77 MeV. The NLEFT procedure used a spherical wall radius of 36 fm.

After adding the centrifugal term, the depth  $V_d$  for  $\ell = 2$  is significantly less than that of  $\ell = 0$ , which is typically not observed in case of other *Ansätze* for the screened Coulomb potential [18,24]. One can observe a repulsive interaction at very short distances, which is due to the downward trend of SPS beyond the peak at 10.88 MeV. The observed experimental resonance energy  $E_r = 3.03$  MeV is again well within the Coulomb barrier height  $V_{CB}$  of 4.9 MeV. The cutoff distance for the potential is obtained at 9.6 fm.

Finally, in the case of  $\ell = 4$ , even though the scattering phase shifts seem have an increasing trend, on close observation one can see a small shift at higher energies towards peaking. In fact, at even higher energies than those considered in this work, one would find scattering phase shifts to peak and have a decreasing trend [39], as observed in case of the  $\ell = 2$  channel. So, one would expect that there would be a relatively small repulsive behavior that would set in even for this channel and is observed in the case of the reference potential approach. Once again, the resonance energy of  $E_r = 11.75$  MeV is observed to be within the range of  $V_{CB}$  values [11.17, 11.16] MeV obtained by us.

#### E. Partial cross section and resonance

The resonances using the  $d\delta/dE$  approach from the obtained scattering phase shifts are found to be 0.1240, 2.95, and

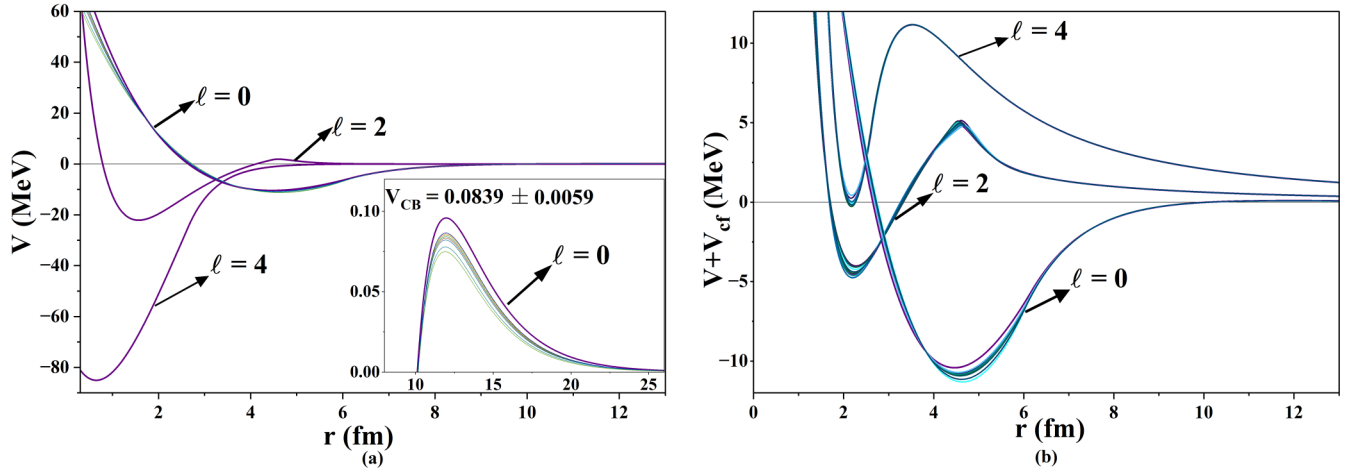


FIG. 3. Inverse potentials for  $\ell = 0, 2, 4$  (a) without and (b) with centrifugal potential term added.

11.89 MeV for  $S$ ,  $D$ , and  $G$  states respectively. The full width at half maximum [FWHM ( $\Gamma'$ )], for  $D$  and  $G$  are determined to be 1.36 and 3.76 MeV respectively. The computed phase shifts are used to determine partial cross sections using

$$\sigma_l = \frac{4\pi}{k^2} (2l + 1) \sin^2 \delta_l(E). \quad (12)$$

In the case of  $\ell = 0$ , there is a sharp resonance behavior very close to 0, and it appears almost like a delta function. As a result, we skipped plotting the partial cross-section for this case. In Fig. 4, the partial cross sections for  $\ell = 2$  and 4 channels are displayed and are seen to be in Breit-Wigner

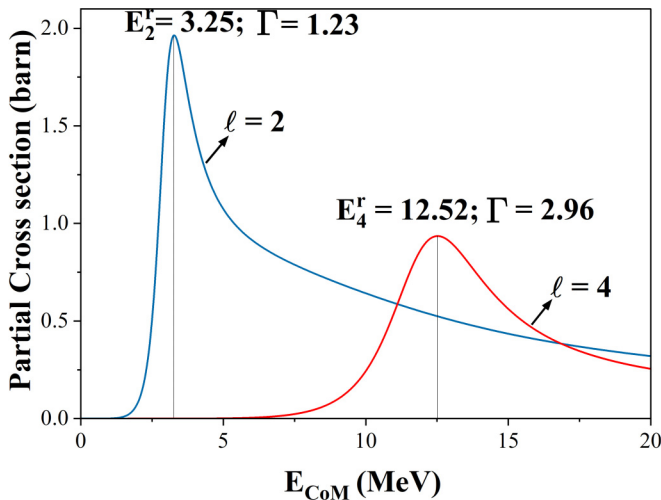


FIG. 4. Partial cross sections for  $\ell = 2$  and 4 for different center-of-mass energies.

form. We obtain the resonance peaks and FWHM  $E_r$  ( $\Gamma$ ) for  $\ell = 2$  and 4 at 3.25 (1.23) MeV and 12.52 (2.96) MeV respectively, as compared to experimental values of 3.03 (1.51) and 11.35 (3.50) [40]. There is a good match between obtained and experimental values as given in Table III.

## VI. DISCUSSION

It is important to mention that the previous efforts to model the Coulomb interaction by incorporating screening by erf() [15–18,23] and the atomic Hulthen [19,24,41] *Ansätze* have given reasonably accurate potentials with only four parameters as compared to the reference potential approach which uses six for the purpose. However, the approximations used in both the erf() [15–18,23] and atomic Hulthen [19,24,41] *Ansätze* have resulted in erroneous function parameters. In the case of the erf() [15–18,23] based *Ansatz*, the integration distance  $r_f$  was abruptly cut off to get the best possible inverse potential. We have observed that this is not an appropriate way to obtain the results, as changing  $r_f$  even by just 1 fm gave very large changes in final phase shifts.

In the case of the atomic Hulthen [19,41] screened potential, the resultant potential for various  $\ell$  channels depends on the choice of screening parameter. Also, this *Ansatz* was unable to pick up the peak in the  $\ell = 2$  channel accurately. It should also be mentioned that considering five-parameter potentials did not enhance the results [24]. So, the constructed inverse potentials in both cases are not independent of the model parameters. On the other hand, the inverse potentials constructed using the reference potential approach in this paper are not at all dependent on the final integration distance. Of course, utilizing six model parameters made a greater span

TABLE III. Obtained resonance energy and full width half maximum using different procedures.

$\ell$ channels	$E_r$ ([40]) (MeV)	$\Gamma$ ([40]) (MeV)	$E_r$ ( $d\delta/dE$ ) (MeV)	$\Gamma'$ (MeV)	$E_r$ (Fig. 4) (MeV)	$\Gamma$ (Fig. 4) (MeV)
$\ell = 0$	0.0918	0.0056	0.124			
$\ell = 2$	3.03	1.51	2.95	1.36	3.25	1.23
$\ell = 4$	11.35	3.50	11.89	3.76	12.52	2.96

of curves available for optimization and hence gave more accurate results as well.

## VII. CONCLUSION

The long-standing challenge of incorporating the long-range coulomb interaction alongside the short-range nuclear interaction for constructing an appropriate scattering potential has been finally solved using a combination of two Morse functions as a reference potential. This could be achieved as a result of our following choices.

- (1) Utilizing the phase function method which directly takes potential as input for determining phase shifts.
- (2) Due to the nature of the Morse function which has all the features observed in scattering phenomena such as strong repulsion at extremely short distances, an attractive nature at intermediate distances, and a quickly decaying tail for the long range.
- (3) The ingenuity of Selg [29,42] to join two Morse functions, with the second one being inverted to create a class of curves that cover all possible scenarios for molecular potentials that have Coulomb barrier.
- (4) Last but not least, a machine-learning-based heuristic algorithm for obtaining global convergence by careful

choice of bounds for the model parameters that result in physically acceptable inverse potentials.

This methodology has been successfully applied to study  $\alpha - \alpha$  scattering of  $\ell = 0, 2, 4$  channels, resulting in the best possible interaction potentials for the available data. We are now looking at other higher channels. Hence, we conclude that the reference potential approach is ideally suited for accurately describing the long-range Coulomb interaction alongside the short-range nuclear interaction for scattering involving charged particles such as  $\alpha - {}^3\text{He}$ ,  $\alpha - {}^3\text{m}$ ,  $\alpha - {}^{12}\text{C}$ ,  $p - {}^{16}\text{O}$ , etc. This procedure could overcome the limitations of previously employed *Ansätze* for the Coulomb interaction.

All codes used in this work are available freely at GitHub [43].

## ACKNOWLEDGMENTS

A.A. acknowledges the financial support provided by the Department of Science and Technology (DST), Government of India through Grant No. DST/INSPIRE Fellowship/2020/IF200538.

The authors declare that they have no conflict of interest.

- 
- [1] E. P. Wigner and L. Eisenbud, Higher angular momenta and long range interaction in resonance reactions, *Phys. Rev.* **72**, 29 (1947).
  - [2] *The J-Matrix Method: Developments and Applications*, edited by A. D. Alhaidari, H. A. Yamani, E. J. Heller, and M. S. Abdelmonem (Springer, Dordrecht, 2008).
  - [3] R. S. Mackintosh, Inverse scattering: applications to nuclear physics, [arXiv:1205.0468](https://arxiv.org/abs/1205.0468).
  - [4] A. Khachi, L. Kumar, A. Awasthi, and O. S. K. S. Sastri, Inverse potentials for all channels of neutron-proton scattering using reference potential approach, *Phys. Scr.* **98**, 095301 (2023).
  - [5] F. Calogero, *Variable Phase Approach to Potential Scattering* (Elsevier, Amsterdam, 1967).
  - [6] V. V. Babikov, The phase-function method in quantum mechanics, *Sov. Phys. Usp.* **10**, 271 (1967).
  - [7] O. S. K. S. Sastri, A. Khachi, and L. Kumar, An innovative approach to construct inverse potentials using variational monte-carlo and phase function method: Application to np and pp scattering, *Braz. J. Phys.* **52**, 58 (2022).
  - [8] V. A. Marchenko, Certain problems in the theory of second-order differential operators, *Dokl. Akad. Nauk SSSR* **72**, 457 (1950).
  - [9] G. Balassa, Estimating scattering potentials in inverse problems with Volterra series and neural networks, *Eur. Phys. J. A* **58**, 186 (2022).
  - [10] Q. Ren, H. Cheng, and H. Han, Research on machine learning framework based on random forest algorithm, *AIP Conf. Proc.* **1820**, 080020 (2017).
  - [11] M. Mitchell, *An Introduction to Genetic Algorithms* (MIT Press, Cambridge, 1998).
  - [12] R. Zemel and T. Pitassi, A gradient-based boosting algorithm for regression problems, *Advances in Neural Information Processing Systems*, edited by T. Leen, T. Dietterich, and V. Tresp (MIT Press, 2000), Vol. 13, pp. 696–702.
  - [13] M. Selg, A practical method for constructing a reflectionless potential with a given energy spectrum, *Proc. Estonian Acad. Sci.* **65**, 358 (2016).
  - [14] J. R. Taylor, A new rigorous approach to coulomb scattering, *Nuovo Cimento B: Series 11* **23**, 313 (1974).
  - [15] S. Ali and A. Bodmer, Phenomenological  $\alpha - \alpha$  potentials, *Nucl. Phys.* **80**, 99 (1966).
  - [16] B. Buck, H. Friedrich, and C. Wheatley, Local potential models for the scattering of complex nuclei, *Nucl. Phys. A* **275**, 246 (1977).
  - [17] M. Odsuren, K. Katō, G. Khuukhenkhuu, and S. Davaa, Scattering cross section for various potential systems, *Nucl. Eng. Technol.* **49**, 1006 (2017).
  - [18] A. Khachi, L. Kumar, and O. S. K. S. Sastri, Alpha-alpha scattering potentials for various  $\ell$ -channels using phase function method, *Phys. At. Nucl.* **85**, 382 (2022).
  - [19] J. Bhoi and U. Laha, Elastic scattering of light nuclei through a simple potential model, *Phys. At. Nucl.* **79**, 370 (2016).
  - [20] L. Kumar, A. Khachi, A. Sharma, and O. S. K. S. Sastri, P & D inverse potentials for proton-proton scattering, *Proc. DAE Symp. Nucl. Phys.* **66**, 579 (2022).
  - [21] S. Awasthi and O. S. K. S. Sastri, Real and imaginary phase shifts for nucleon-deuteron scattering using phase function method, [arXiv:2304.10478](https://arxiv.org/abs/2304.10478).
  - [22] L. Kumar, S. Awasthi, A. Khachi, and O. S. K. S. Sastri, Phase shift analysis of light nucleon-nucleus elastic scattering using reference potential approach, [arXiv:2209.00951](https://arxiv.org/abs/2209.00951).
  - [23] A. Khachi, O. S. K. S. Sastri, L. Kumar, and A. Sharma, Phase shift analysis for alpha-alpha elastic scattering using phase

- function method for Gaussian local potential, *J. Nucl. Phys. Mater. Sci. Radiat. Appl.* **9**, 1 (2021).
- [24] A. Awasthi and O. S. K. S. Sastri, Comparative Study of alpha-alpha interaction potentials constructed using various phenomenological models, [arXiv:2307.13207](https://arxiv.org/abs/2307.13207).
- [25] S. Elhatisari, D. Lee, G. Rupak, E. Epelbaum, H. Krebs, T. A. Lähde, T. Luu, and U.-G. Meißner, Ab initio alpha-alpha scattering, *Nature (London)* **528**, 111 (2015).
- [26] S. Elhatisari, T. A. Lähde, D. Lee, U.-G. Meißner, and T. Vonk, Alpha-alpha scattering in the multiverse, *J. High Energy Phys.* **02** (2022) 001.
- [27] B. Behzadmoghaddam, M. Radin, and S. Bayegan, The  $^1S_0$  channel of proton-proton scattering in new chiral effective field theory power counting, *Sci. Rep.* **13**, 7041 (2023).
- [28] T. A. Lähde and U.-G. Meißner, *Nuclear Lattice Effective Field Theory: An Introduction*, Lecture Notes in Physics (Springer, Berlin, 2019), Vol. 957.
- [29] M. Selg, Formation and rotational-vibrational relaxation of diatomic rare gas excimers, *Phys. Scr.* **52**, 287 (1995).
- [30] M. Selg, Reference potential approach to the quantum-mechanical inverse problem: I. calculation of phase shift and Jost function, [arXiv:quant-ph/0506064](https://arxiv.org/abs/quant-ph/0506064).
- [31] M. Selg, Numerically complemented analytic method for solving the time-independent one-dimensional Schrödinger equation, *Phys. Rev. E* **64**, 056701 (2001).
- [32] M. Selg, Visualization of rigorous sum rules for Franck-Condon factors: spectroscopic applications to Xe<sub>2</sub>, *J. Mol. Spectrosc.* **220**, 187 (2003).
- [33] B. Talukdar, D. Chattarji, and P. Banerjee, A generalized approach to the phase-amplitude method, *J. Phys. G* **3**, 813 (1977).
- [34] G. Sett, U. Laha, and B. Talukdar, Phase-function method for Coulomb-distorted nuclear scattering, *J. Phys. A: Math. Gen.* **21**, 3643 (1988).
- [35] A. Lambora, K. Gupta, and K. Chopra, Genetic algorithm—a literature review, in *2019 International Conference on Machine Learning, Big Data, Cloud and Parallel Computing (COMITCon)* (IEEE, Piscataway, NJ, 2019), pp. 380–384.
- [36] X.-S. Yang, *Engineering Optimization: An Introduction with Metaheuristic Applications* (John Wiley & Sons, New York, 2010).
- [37] S. Mirjalili, *Evolutionary Algorithms and Neural Networks: Theory and Applications*, Lecture Notes in Physics (Springer, Berlin, 2018), Vol. 780.
- [38] W. S. Chien and R. E. Brown, Study of the  $\alpha + \alpha$  system below 15 MeV (c.m.), *Phys. Rev. C* **10**, 1767 (1974).
- [39] S. Afzal, A. Ahmad, and S. Ali, Systematic survey of the  $\alpha - \alpha$  interaction, *Rev. Mod. Phys.* **41**, 247 (1969).
- [40] D. Tilley, J. Kelley, J. Godwin, D. Millener, J. Purcell, C. Sheu, and H. Weller, Energy levels of light nuclei  $A = 8, 9, 10$ , *Nucl. Phys. A* **745**, 155 (2004).
- [41] J. Bhoi, R. Upadhyay, and U. Laha, Parameterization of nuclear Hulthén potential for nucleus-nucleus elastic scattering, *Commun. Theor. Phys.* **69**, 203 (2018).
- [42] M. Selg, Quantum-mechanical treatment of the fine structure of molecular-type absorption spectra of rare gases. application to Xe<sub>2</sub>, *Phys. Scr.* **47**, 769 (1993).
- [43] [https://github.com/Arushiabhi/Phase\\_Shift.git](https://github.com/Arushiabhi/Phase_Shift.git)